

HIGH-PRECISION PREDICTION FOR MULTI-SCALE PROCESSES AT THE LHC*

RENE PONCELET

Institute of Nuclear Physics Polish Academy of Sciences
Radzikowskiego 152, 31-342, Kraków, Poland

*Received 2 May 2024, accepted 3 June 2024,
published online 5 August 2024*

Comparisons of higher-order predictions within the Standard Model of Particle Physics (SM) to data are central to high-energy collider experiments like the Large Hadron Collider (LHC). Processes with multiple kinematic scales, such as multi-jet and prompt photon production, provide a unique possibility for probing Quantum Chromodynamics (QCD). These processes directly test perturbative QCD and can be used to extract fundamental parameters like the strong coupling constant and to search for BSM physics. Recent developments enabled lifting three-jet, photon + two-jet, photon-pair + jet, and three-photon cross sections to QCD's next-to-next-to-leading order (NNLO). This contribution presents phenomenological results at NNLO QCD for the three-jet and photon plus two-jet production.

DOI:10.5506/APhysPolBSupp.17.5-A4

1. Introduction

Tests of perturbative QCD are a staple of the LHC physics program. Processes at high energy allow for comparisons between data and numerical predictions derived from perturbation theory. Calculations performed at leading or next-to-leading perturbative orders (LO and NLO) can readily be obtained from public and automated software, but suffer from large corrections from missing higher orders, mostly estimated through the dependence on non-physical scales. Therefore, computations performed at NNLO or even next-to-next-to-next-to-leading are needed to stabilize the perturbative series such that comparison to data can be performed reliably. For Standard Model processes with low multiplicity, *e.g.* one or two particles in the final state at leading-order, next-to-next-to-leading order have become the state-of-the-art in the past two decades. This has been driven by the

* Presented at the 30th Cracow Epiphany Conference on *Precision Physics at High Energy Colliders*, Cracow, Poland, 8–12 January, 2024.

development of subtraction and slicing methods to control the infrared singularities of real emission contributions and improved techniques for loop amplitude calculations. A review of these achievements can be found in Ref. [1].

The methods' extensions to higher multiplicity processes, *i.e.* processes with more kinematical scales, faced two substantial bottlenecks: Firstly, the computational efficiency and generality of the subtraction and slicing methods had to be improved to deal with the increasing complexity of the phase space and infrared singularity structure. Secondly, the required two-loop amplitudes, whose structures are increasingly more complex, had to be calculated. Recent advances on both fronts have made the computation of NNLO QCD corrections possible for processes with three massless final-state particles at the tree level: three-photon production [2–6], di-photon + jet [7–11], photon + di-jet [12], and three-jet production [13–16] (also the purely gluonic component [17]). Also, the first computations of processes where one of the three particles has a non-vanishing invariant mass have been performed [18–23].

This contribution highlights some of the results for three-jet and photon + di-jet production, focusing on the phenomenological results and first comparisons to data.

2. Computational methods and setup

The presented calculations have been performed in the formalism of collinear factorisation, where the hadronic cross section of production of a final-state X in the scattering of two hadrons h_1 and h_2 is written as a convolution of parton distribution functions (PDFs) ($\phi_{i,h}(x, \mu_F)$) with the partonic cross section $\hat{\sigma}$ for producing the same final state

$$\sigma_{h_1 h_2 \rightarrow X} = \sum_{ij} \int_0^1 dx_1 dx_2 \phi_{i,h_1}(x_1, \mu_F^2) \phi_{j,h_2}(x_2, \mu_F^2) \hat{\sigma}_{ij \rightarrow X}(\mu_R^2, \mu_F^2). \quad (1)$$

This holds up to power corrections in λ_{QCD}/Q . Here, μ_F denotes the factorisation and μ_R the renormalisation scale. The partonic cross section $\hat{\sigma}$ can be expanded in the strong coupling constant

$$\hat{\sigma}_{ab \rightarrow X} = \hat{\sigma}_{ab \rightarrow X}^{(0)} + \alpha_S^1 \hat{\sigma}_{ab \rightarrow X}^{(1)} + \alpha_S^2 \hat{\sigma}_{ab \rightarrow X}^{(2)} + \mathcal{O}(\alpha_S^3). \quad (2)$$

The arising infra-red singularities beyond the tree-level approximation in this series cancel in sufficiently inclusive quantities; their treatment in calculations showed in this contribution is done within the sector-improved

residue subtraction scheme [24–26] as implemented in the C++ code `Stripper`. All necessary tree-level amplitudes are evaluated using the AvH library [27]. The one-loop amplitudes that start to contribute at the first relative order in α_S are evaluated using the `OpenLoops2` software [28].

No automated numerical method is currently available for the two-loop amplitudes, starting to contribute at order $\mathcal{O}(\alpha_S^2)$. They are, therefore, derived case-by-case in analytical computations. All necessary massless five-point helicity amplitudes have been obtained in a series of publications by different groups, first in the planar or leading-colour approximation [3, 4, 7, 8, 13] and, more recently, with the complete colour dependence [6, 9, 11, 12, 29]. The amplitudes are represented in terms of so-called ‘Pentagon’-functions [30–34], rational coefficient functions of the external kinematic invariants and phase factors. For the phenomenological applications presented here, the amplitudes have been implemented in an independent C++ code. The only exception is the set of amplitudes for three-jet production, where the public code presented in Ref. [14] has been employed. Both implementations allow for a stable and fast evaluation of the amplitudes during the integration of the cross section.

3. Three-jet production

Tests of perturbative QCD and measurements of the strong coupling constant using multi-jet rates and event-shape observables have a long history. At lepton colliders, these measurements present the first direct confirmations of the validity of QCD and allow for a precise extraction of the fundamental parameters of the theory, *i.e.* the coupling constant α_S and the number of colours. At hadron–hadron colliders, the main challenge in achieving competitive measurements despite the enormous amount of available data is the large theoretical uncertainty in perturbative calculations of the relevant observables. In particular, the dependence on unphysical scales is by far the largest uncertainty in the extraction of α_S from jet rates or event-shapes. This section reviews some of the results for the novel NNLO QCD corrections obtained in Refs. [15, 16] overcoming these bottlenecks. Also, a complete overview of the technical details can be found here.

The basic quantity is the (differential) ratio of the inclusive three-jet production rate to the inclusive di-jet–jet production rate

$$\frac{dR_{3/2}(\mu_R, \mu_F)}{dX} = \frac{d\sigma_3(\mu_R, \mu_F)/dX}{d\sigma_2(\mu_R, \mu_F)/dX}. \quad (3)$$

Here, $d\sigma_n$ is defined as the (differential) n -jet cross section for having at least n reconstructed anti- k_T jets fulfilling analysis-dependent phase-space

requirements. The renormalisation and factorisation scales in these computations have been set to the scalar sum partonic transverse momenta

$$\mu_R = \mu_F = \hat{H}_T = \sum_{i \in \text{partons}} p_{T,i}, \quad (4)$$

possibly divided by some constant rational factor. The PDFs are evaluated using the LHAPDF package [35]; if not specified otherwise, the NNPDF3.1 PDF [36] parametrization is used. Estimates of uncertainties from missing higher orders (MHO) are obtained from conventional 7-point scale variations by a factor of 2, *i.e.* scale choices within the constraints $1/2 \leq \mu_F/\mu_R \leq 2$.

As an example, the left-hand side in Fig. 1 shows the differential $R_{3/2}$ -ratio with respect to $H_T = \sum_{i \in \text{jets}} p_T(j_i)$ for 13 TeV proton–proton collisions. The $\mathcal{O}(1)$ differences between LO and NLO QCD indicate that higher-order corrections are important to describe this observable. At NLO QCD, the MHO uncertainty estimates are of $\mathcal{O}(20\%)$ which cover the actual NNLO QCD corrections, which are, for high values of H_T (> 800 GeV), about 3–5%. Estimates of corrections from beyond NNLO QCD are tiny and not visibly resolved. The feature in the first bin can be traced back to sensitivity to the phase-space boundaries and corresponding enhancements and instabilities.

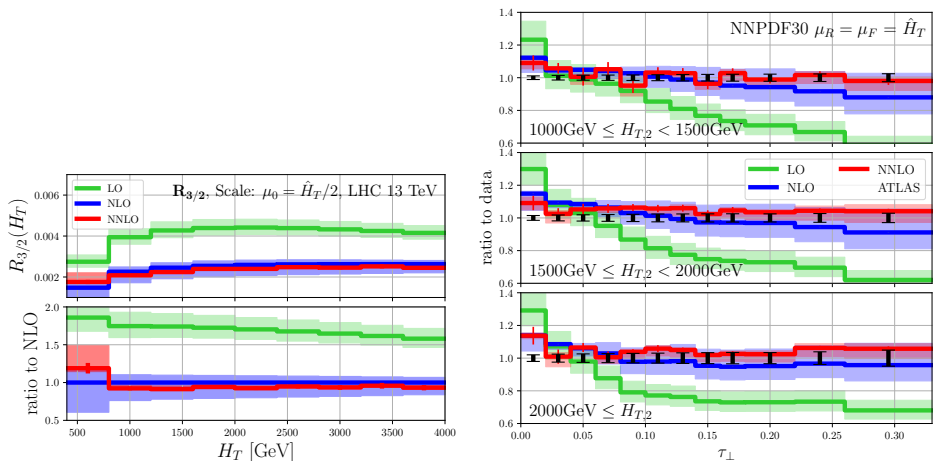


Fig. 1. (Colour on-line) Perturbative predictions through LO (green/light grey), NLO (blue/dark grey), and NNLO (red/grey) QCD at 13 TeV. Bands indicate estimates of corrections from missing higher orders. Left: plot of $dR_{3,2}/dH_T$, the upper panel shows absolute values, and the lower panel ratios with respect to NLO QCD. Further details in Ref. [15]. Right: plot of the transverse thrust observable τ_\perp in different regions of $H_{T,2}$ compared to ATLAS data (black) [37]. For details, refer to Ref. [16].

Event shape observables have been designed to study the geometry of events as a whole, not only a mere sum of its constituents. The (transverse) ‘thrust’-observable T_{\perp} (or rather $\tau_{\perp} = 1 - T_{\perp}$) [38, 39], for example, separates isotropic from anisotropic back-to-back configurations and is defined by

$$T_{\perp} = \max_{\hat{n}_{\perp}} \left\{ \frac{\sum_i |\vec{p}_{T,i} \cdot \hat{n}_{\perp}|}{\sum_i |\vec{p}_{T,i}|} \right\}, \quad (5)$$

where the \hat{n}_{\perp} that maximises the expression is called the transverse thrust axis. This quantity (together with several other event shapes) has been measured by the ATLAS Collaboration in regions of $H_{T,2} = p_{T,1} + p_{T,2}$ and compared to predictions from the Monte Carlo simulations in Ref. [37]. While the overall description through the simulation is reasonable, several differences in shapes and normalization motivated the inclusion of NNLO QCD corrections in Ref. [16]. For example, the right-hand side of Fig. 1 shows perturbative QCD predictions for this observable comparison with the ATLAS data. The description of the data improves with increasing perturbative order. Also clearly visible is the significant reduction of the MHO uncertainty estimates at NNLO QCD. The data is fully compatible with these uncertainties (taking into account the remaining statistical uncertainties, shown as vertical bars).

The last highlighted multi-jet observable is the transverse energy–energy correlator (TEEC) [40, 41]. Perturbative QCD results obtained in [16] can be found on the left-hand side of Fig. 2. Similar to τ_T , a clear reduction of perturbative corrections and MHO uncertainties can be observed when going to NNLO QCD. These results have been used in a refined form in an

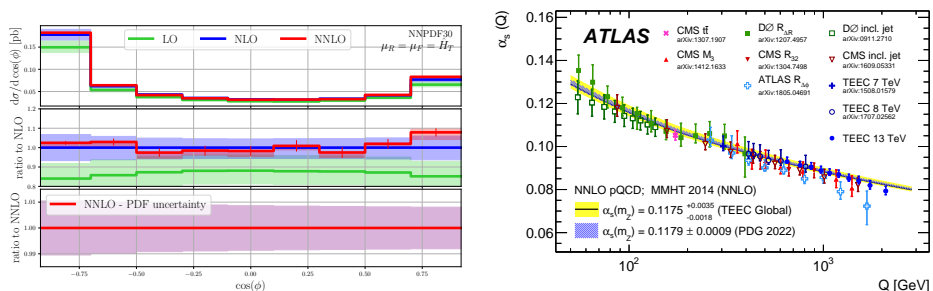


Fig. 2. (Colour on-line) Left: plots of perturbative predictions (LO — green/light grey, NLO — blue/dark grey, NNLO — red/grey) for the TEEC event shape observable: the upper panel shows the absolute distribution, the central panel the results as a ratio to NLO QCD, and the lower panel the PDF uncertainties for reference. For details, see Ref. [16]. Right: the extraction of the strong coupling constant as a function of the energy scale, taken from Ref. [41].

experimental publication [41] performing a measurement of the TEEC from multi-jet events to not only make a comparison between theory and data but also to extract α_S as a function of the event's energy scale, see the right-hand side of Fig. 2. Similar extractions have been performed previously using only NLO QCD accuracy but had up to 3 times larger theory uncertainties, which is the dominating uncertainty.

4. Prompt photon production in association with jets

The second example of a massless two-to-three process in this contribution is the production of an isolated photon associated with a pair of jets [12]. Photon production in hadron-hadron collisions is an important probe of QCD and possesses a rich phenomenology. From the perspective of perturbative QCD, highly energetic prompt photons are of particular interest. There are two main mechanisms to produce prompt photons: fragmentation and direct photon production. To identify prompt photons, isolation criteria, *e.g.* cuts on the hadronic activity in a cone around candidate photons, are used to suppress background contributions such as those from hadron decays. Unfortunately, these experimental criteria are not infra-red-safe in perturbative calculations and require either the inclusion of fragmentation in the calculation or a prescription to remove or suppress these contributions. A simple but phenomenologically effective method is the smooth or hybrid cone isolation [42, 43]. In Ref. [12], a hybrid cone isolation prescription has been employed. Further details about the calculations, such as phase-space definition and observables, can also be found therein.

Figure 3 shows two differential distributions, the transverse energy spectrum of the photon $E_T(\gamma)$ and the transverse momentum distribution of the two leading jets p_T^{jet} (both jets are accounted for in the same histogram). The perturbative computations are compared to data measured by the ATLAS Collaboration [44]. The perturbative corrections indicate a well-behaving perturbative series, *i.e.* the corrections are getting smaller, and the scale uncertainties are reduced. The NNLO QCD prediction describes the data well. Besides the perturbative corrections, two different scale choices, $\mu = H_T = E_T(\gamma) + p_T(j_1) + p_T(j_2)$ and $\mu = E_T(\gamma)$ are compared. In both distributions, one observes that the H_T scale has a better perturbative convergence behaviour and, therefore, seems to represent the physical scales much better than $E_T(\gamma)$.

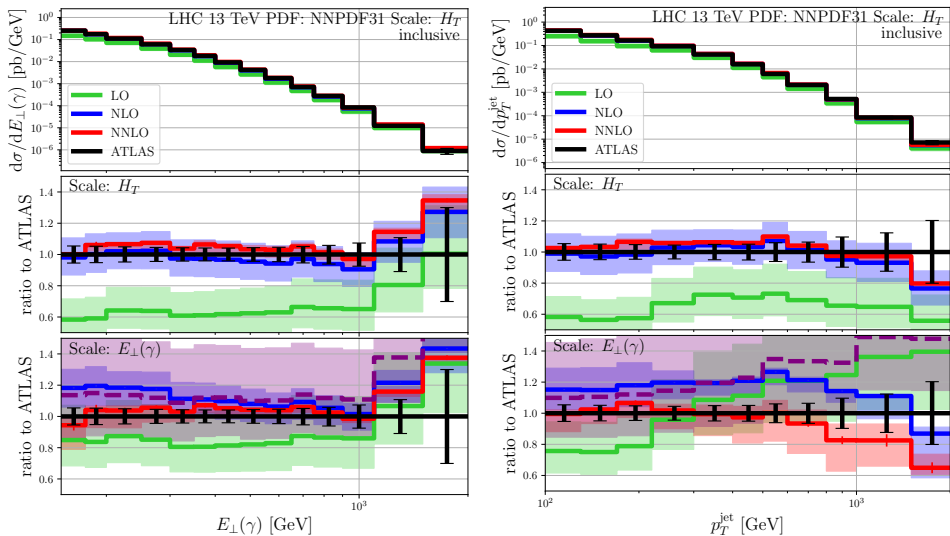


Fig. 3. (Colour on-line) Plot of differential distributions in photon plus di-jet production computed in perturbation theory (LO — green/light grey, NLO — blue/dark grey, NNLO — red/grey), compared to ATLAS data (black) and Monte Carlo predictions (purple dashed line). For details, see Ref. [12].

5. Summary and outlook

In recent years, the computation of second-order QCD corrections to the cross section of all massless two-to-three processes at the LHC have been performed: $pp \rightarrow \gamma\gamma\gamma$ [2], $pp \rightarrow \gamma\gamma j$ [10], $pp \rightarrow \gamma jj$ [12], and $pp \rightarrow jjj$ [15, 16]. These computations are complete in $n_f = 5$ massless QCD as far as the double real and real-virtual corrections are concerned, and have employed a planar/leading-colour approximation for the double virtual contributions. This is except for [12], which, besides being the first computation with complete double virtual amplitudes, demonstrated that this approximation was well justified. The results have been compared to data, and agreement within the uncertainty has been found. The results for three-jet production have been used by the ATLAS Collaboration to extract the strong coupling from TEECs for the first time using NNLO QCD accurate theory.

The limitation of the planar approximation for double virtual corrections has been lifted, and all relevant amplitudes are available in complete form. Their inclusion in phenomenological studies is a logical next step. Processes with a single massive (colour-less) particle, such as $V + 2j$ processes, are the natural next challenge, for which first steps have been taken [21, 22]. Further progress is mostly tied to the computation of the respective two-loop amplitudes.

This work was partly supported by grant No. 2019/35/B/ST2/03531 of the National Science Centre (NCN), Poland.

REFERENCES

- [1] T. Gehrmann, B. Malaescu, *Annu. Rev. Nucl. Part. Sci.* **72**, 233 (2022).
- [2] H.A. Chawdhry, M. Czakon, A. Mitov, R. Poncelet, *J. High Energy Phys.* **2020**, 057 (2020).
- [3] S. Abreu, B. Page, E. Pascual, V. Sotnikov, *J. High Energy Phys.* **2021**, 078 (2021).
- [4] H.A. Chawdhry, M. Czakon, A. Mitov, R. Poncelet, *J. High Energy Phys.* **2021**, 150 (2021).
- [5] S. Kallweit, V. Sotnikov, M. Wiesemann, *Phys. Lett. B* **812**, 136013 (2021).
- [6] S. Abreu *et al.*, *SciPost Phys.* **15**, 157 (2023).
- [7] B. Agarwal, F. Buccioni, A. von Manteuffel, L. Tancredi, *J. High Energy Phys.* **2021**, 201 (2021).
- [8] H.A. Chawdhry, M. Czakon, A. Mitov, R. Poncelet, *J. High Energy Phys.* **2021**, 164 (2021).
- [9] B. Agarwal, F. Buccioni, A. von Manteuffel, L. Tancredi, *Phys. Rev. Lett.* **127**, 262001 (2021).
- [10] H.A. Chawdhry, M. Czakon, A. Mitov, R. Poncelet, *J. High Energy Phys.* **2021**, 093 (2021).
- [11] S. Badger *et al.*, *J. High Energy Phys.* **2021**, 083 (2021).
- [12] S. Badger *et al.*, *J. High Energy Phys.* **2023**, 071 (2023).
- [13] S. Abreu *et al.*, *J. High Energy Phys.* **2018**, 116 (2018).
- [14] S. Abreu *et al.*, *J. High Energy Phys.* **2021**, 095 (2021).
- [15] M. Czakon, A. Mitov, R. Poncelet, *Phys. Rev. Lett.* **127**, 152001 (2021); *Erratum ibid.* **129**, 119901 (2022).
- [16] M. Alvarez *et al.*, *J. High Energy Phys.* **2023**, 129 (2023).
- [17] X. Chen *et al.*, *J. High Energy Phys.* **2022**, 099 (2022).
- [18] S. Badger, H.B. Hartanto, S. Zoia, *Phys. Rev. Lett.* **127**, 012001 (2021).
- [19] S. Badger, H.B. Hartanto, J. Kryś, S. Zoia, *J. High Energy Phys.* **2021**, 012 (2021).
- [20] S. Abreu *et al.*, *J. High Energy Phys.* **2022**, 042 (2022).
- [21] H.B. Hartanto, R. Poncelet, A. Popescu, S. Zoia, *Phys. Rev. D* **106**, 074016 (2022).
- [22] L. Buonocore *et al.*, *Phys. Rev. D* **107**, 074032 (2023).
- [23] S. Badger, H.B. Hartanto, J. Kryś, S. Zoia, *J. High Energy Phys.* **2022**, 035 (2022).
- [24] M. Czakon, *Phys. Lett. B* **693**, 259 (2010).

- [25] M. Czakon, D. Heymes, *Nucl. Phys. B* **890**, 152 (2014).
- [26] M. Czakon, A. van Hameren, A. Mitov, R. Poncelet, *J. High Energy Phys.* **2019**, 262 (2019).
- [27] M. Bury, A. van Hameren, *Comput. Phys. Commun.* **196**, 592 (2015).
- [28] F. Buccioni *et al.*, *Eur. Phys. J. C* **79**, 866 (2019).
- [29] B. Agarwal *et al.*, *Phys. Rev. D* **109**, 094025 (2024), [arXiv:2311.09870 \[hep-ph\]](https://arxiv.org/abs/2311.09870).
- [30] D. Chicherin *et al.*, *Phys. Rev. Lett.* **123**, 041603 (2019).
- [31] D. Chicherin, V. Sotnikov, *J. High Energy Phys.* **2020**, 167 (2020).
- [32] D.D. Canko, C.G. Papadopoulos, N. Syrrakos, *J. High Energy Phys.* **2021**, 199 (2021).
- [33] S. Abreu, H. Ita, B. Page, W. Tschernow, *J. High Energy Phys.* **2022**, 182 (2022).
- [34] D. Chicherin, V. Sotnikov, S. Zoia, *J. High Energy Phys.* **2022**, 096 (2022).
- [35] A. Buckley *et al.*, *Eur. Phys. J. C* **75**, 132 (2015).
- [36] NNPDF Collaboration (R.D. Ball *et al.*), *Eur. Phys. J. C* **77**, 663 (2017).
- [37] ATLAS Collaboration (G. Aad *et al.*), *J. High Energy Phys.* **2021**, 188 (2021); *Erratum ibid.* **2021**, 053 (2021).
- [38] S. Brandt, C. Peyrou, R. Sosnowski, A. Wroblewski, *Phys. Lett.* **12**, 57 (1964).
- [39] E. Farhi, *Phys. Rev. Lett.* **39**, 1587 (1977).
- [40] A. Ali, E. Pietarinen, W.J. Stirling, *Phys. Lett. B* **141**, 447 (1984).
- [41] ATLAS Collaboration (G. Aad *et al.*), *J. High Energy Phys.* **2023**, 085 (2023).
- [42] S. Frixione, *Phys. Lett. B* **429**, 369 (1998).
- [43] F. Siegert, *J. Phys. G: Nucl. Part. Phys.* **44**, 044007 (2017).
- [44] ATLAS Collaboration (G. Aad *et al.*), *J. High Energy Phys.* **2020**, 179 (2020).